Acid Zeolites as Electron Acceptors. Use of Thianthrene Radical Cation as a Probe

Avelino Corma,* Vicente Fornés, Hermenegildo García,* Vicente Martí, and Miguel A. Miranda

Instituto de Tecnología Química UPV-CSIC, Universidad Politécnica de Valencia, Apartado 22012, 46071-Valencia, Spain

Received May 12, 1995. Revised Manuscript Received August 11, 1995[⊗]

Adsorption of thianthrene (Th) within a series of acid zeolites with medium, large, and extra large pore size including novel zeotypes MCM-22 and MCM-41 led as a general process to the generation of Th radical cation ($Th^{\bullet+}$). This species was unambiguously characterized by UV/vis diffuse reflectance, EPR, and IR spectroscopies. In the case of Y and β hosts, dimeric aggregates could be observed. Vapor phase incorporation of Th at 473 K under Ar atmosphere was found to be the most clean and convenient adsorption procedure. Ambient moisture was the main factor responsible for aging of $Th^{\bullet+}$ composites. This process was totally reversible. This result suggest that reversible complexation of $Th^{\bullet+}$ with H_2O is the process ocurring at initial stages. On the other hand, oxygen is not necessary for the formation of $Th^{\bullet+}$. The Brönsted and Lewis population of the acid sites were characterized by IR spectroscopy, following the pyridine adsorption-desorption method. Brönsted zeolites prepared by removal of the extraframework Al are active to generate $Th^{\bullet+}$. Neutralization of Brönsted sites by Na^+ exchange fully deactivated the solids despite of the presence of residual Lewis sites. Th oxidation must occur predominantly on the zeolite Brönsted sites.

Introduction

Recent studies have revealed that radical cations of electron rich olefins,[1-5] dienes,[6-8] conjugated α,ω--diphenyl polyenes,[6] arenes,[2,9,10] polythiophenes,[11] amines,[12,13] and even saturated hydrocarbons[14] can be spontaneously generated by mere adsorption onto dehydrated zeolites at room temperature.

This simple procedure to generate radical cations by incorporation within zeolites might constitute a suitable methodology to study the physical properties and control the chemical reactivity of these elusive intermediates. Thus, the zeolite framework would provide a rigid matrix to isolate the radical cations, while the intense electrostatic fields experienced inside the micropores of zeolites would contribute to stabilize positively charged species[15] and in particular radical ion pairs.[16-18] Besides, the shape, size, and topology of the zeolite framework can impose geometrical constraints on the reactivity of the confined radical cations.[19]

However, in order to establish the general scope of this method, some important points need to be addressed. Thus, the exact nature and location of the electron acceptor sites in zeolites are still a matter of controversy.[20] Therefore, the efficiency of a particular zeolite sample as radical cation generator cannot be easily anticipated, and no zeolite treatments are available to control the population and the strength of the oxidizing sites. Moreover, while the chemical composition of zeolites can be varied independently of their crystalline structure, it is still confusing why some types of zeolites seem to be unable to generate radical cations, while others with similar physicochemical parameters exhibit a high activity. This is the case of the faujasites, which were found to be inactive for the generation of radical cations from α,ω-diphenyl polyenes.[21]

Studies on the influence of the nature of charge-balancing alkaline cation have shown that they do not play a pivotal role in the electron acceptor ability of zeolites. By contrast, a relationship between the aluminum content of the zeolite and the population of oxidizing sites has been roughly inferred, since purely siliceous materials are apparently unable to generate radical cations.[1,21-23]

[⊗] Abstract published in *Advance ACS Abstracts,* September 15, 1995.

(1) Pollack, S. S.; Sprecher, R. F.; Frommell, E. A. *J. Mol. Catal.* **1991**, *66*, 195-203.
(2) Rhodes, C. J. *J. Chem. Soc., Faraday Trans.* **1991**, *87*, 3179-3184.
(3) Roduner, E.; Wu, L. M.; Crockett, R.; Rhodes, C. J. *Catal. Lett.* **1992**, *14*, 373-379.
(4) Rhodes, C. J. *Colloids Surf. A* **1993**, *72*, 111-118.
(5) Crockett, R.; Roduner, E. *J. Chem. Soc., Perkin Trans. 2* **1993**, 1503-1509.
(6) Ramamurthy, V.; Caspar, J. V.; Corbin, D. R. *J. Am. Chem. Soc.* **1991**, *113*, 594-600.
(7) Rhodes, C. J.; Standing, M. *J. Chem. Soc., Perkin Trans. 2* **1992**, 1455-1460.
(8) Roduner, E.; Crockett, R.; Wu, L. M. *J. Chem. Soc., Faraday Trans.* **1993**, *89*, 2101-2105.
(9) Chen, F. R.; Fripiat, J. J. *J. Phys. Chem.* **1992**, *96*, 819-823.
(10) Liu, X. S.; Thomas, J. K. *Langmuir* **1993**, *9*, 727-732.
(11) Caspar, J. V.; Ramamurthy, V.; Corbin, D. R. *J. Am. Chem. Soc.* **1991**, *113*, 600-610.
(12) Chen, F. R.; Fripiat, J. J. *Proc. Ninth International Zeolite Conference*, von Ballmoos, R., Higgins, J. B., Treacy, M. M. J., Eds.; Butterworth-Heinemann: Montreal, 1992; pp 603-610.
(13) Brunel, D.; Nagy, J. B.; Daelen, G.; Derouane, E. G.; Geneste, P.; Vanderveken, D. J. *Appl. Catal. A* **1993**, *99*, 9-20.
(14) Chen, F. R.; Fripiat, J. J. *J. Phys. Chem.* **1993**, *97*, 5796-5797.
(15) Yoon , K. B. *Chem. Rev.* **1993**, *93*, 321-339.
(16) Sankararaman, S.; Yoon, K. B.; Yabe, T.; Kochi, J. K. *J. Am. Chem. Soc.* **1991**, *113*, 1419-1421.
(17) Dutta, P. K.; Turbeville, W. *J. Phys. Chem.* **1992**, *96*, 9410-9416.
(18) Dutta, P. K.; Borja, M. *J. Chem. Soc., Chem. Commun.* **1993**, 1568-1569.
(19) Turro, N. J.; García-Garibay, M. A. In *Photochemistry in Organized and Constrained Media*; Ramamurthy, V., Ed.; VCH: New York, 1991; pp 1-38.
(20) Cano, M. L.; Corma, A.; Fornés, V.; García, H.; Miranda, M. A. *J. Phys. Chem.* **1995**, *99*, 4241 and references therein.

0897-4756/95/2807-2136$09.00/0

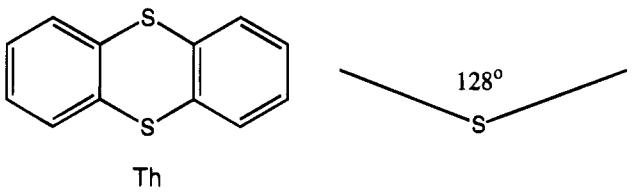

Th

Figure 1. Chemical structure of thianthrene including C–S–C angle.

We have previously examined the ability of several large pore zeolites to generate organic cations from their neutral precursors, a process thought to involve radical cations as intermediates.[20]

In the present work, we have performed the adsorption of thianthrene (Th) onto a series of mono- and tridimensional medium, large, and extra large[24] pore acid zeolites. Th forms one of the best-documented radical cations ($Th^{\bullet+}$).[25-27] This species can be generated by dissolving Th in a variety of strong Brönsted and Lewis acids including H_2SO_4, $HClO_4$, CF_3CO_2H, or $AlCl_3$ and can even be isolated as a moderately stable salt of nonnucleophilic counter-anions like ClO_4^- or BF_4^-.[28,29] The very characteristic absorption spectrum of $Th^{\bullet+}$ allows unambiguously its identification and quantification by UV/vis spectroscopy. Moreover, the exhaustive knowledge of physical and chemical properties of $Th^{\bullet+}$ can be used not only to determine the electron acceptor ability of zeolites, but also to gain a better understanding of the distinctive topological characteristics (size, shape, and mono- or tridirectional network) of the confined spaces experienced by $Th^{\bullet+}$ in each microporous solid. On the other hand, the zeolite structure may impose geometrical restrictions on the chemical behaviour of $Th^{\bullet+}$. Using this species as a probe, we will show herein that the electron acceptor ability is a general property of acid zeolites (Figure 1).

Experimental Section

Acid Zeolites. HY-100 was prepared starting from a commercial NaY (Union Carbide, SK-40) sample by ion exchange using aqueous solutions of NH_4AcO following the protocol previously reported.[30] HY-100-N was obtained from HY-100 by four consecutive cycles consisting of ion exchange at room temperature using a 1 M aqueous solution of NaCl and drying (378 K, 5 h). CsY was obtained from NaY by two successive cycles of ion exchange (353 K, 1 h) using 1 M aqueous solution of $CsNO_3$ and drying (378 K, 5 h); the percentage of Na^+-to-Cs^+ exchange determined by chemical analysis was 78%. HYD was a commercial sample (PQ Industries, CBV720). HYD-W was obtained from a steam dealuminated Y sample by washing exhaustively with $(NH_4)_2SiF_6$. Hβ was obtained by thermal decomposition (773 K, N_2 stream, 2 h) of the tetraethylammonium form of an as-synthesized sample prepared according to the literature.[31] HMor was obtained by treating at 323 K a commercial NaMor (PQ Industries, Si/Al 6) with 1 M hydrochloric acid for 30 min[32] and then washing thoroughly the solid with distilled water until no precipitation of Cl^- took place. HZSM-5 and silicalite were synthesized according to patent literature,[33] and calcined (823 K) to decompose the organic template. MCM-41 was synthesized by using amorphous silica (Aerosil 200, Degussa), a 25% aqueous solution of tetramethylammonium hydroxide, and an aqueous solution of hexadecyltrimethylammonium bromide as templates following reported procedures;[34] the Si:Al ratio of the sample determined by chemical analysis was 95, while the pore diameter measured by Ar adsorption was 3 nm. ZSM-12 and MCM-22 were obtained as previously reported[35-37] by hydrothermal synthesis at 423 K using hexamethyleneimine as template and Si:Al gel ratios of 100 and 15, repectively; these samples were calcined in air at 853 K for 3 h to decompose the organic material and then the H^+ form obtained by two consecutive exchanges (2 M NH_4Cl aqueous solution)–calcination (air, 823 K, 3h) cycles. The offretite sample was kindly provided by Prof. F. Figueras (Montpellier). Silica alumina 25 wt % was purchased from Bayer and the measured external area was 250 m $\times$ g^{-1}.

Adsorption Procedures. When adsorption of Th was performed from organic solutions, a known amount (about 50 mg) was dissolved in the appropriate solvent (25 mL) and the solution was added to the corresponding zeolite (1.00 g), thermally activated (773 K, overnight) just prior its use. The resulting suspension was magnetically stirred at reflux temperature for 1 h. After this time, the solid was centrifuged and washed with fresh solvent (5 mL) at room temperature for 15 min. The combined organic solutions were analyzed by GC-MS (Varian Saturn II, 25 m capillary column 5% phenylmethylsilicone), GC-FTIR (HP 5890 gas chromatograph, same column as GC-MS, coupled with a FT-IR HP 5965A detector) and the residue after solvent removal submitted to a control by ^1H NMR (400 MHz, Varian Unity +).

When adsorption of Th was carried out from the vapor phase, a mixture of Th (50 mg) and the corresponding zeolite (1.00 g) was ground in a morter, placed within a Pyrex reactor and heated up to 473 K under a continuous gas flow.

Characterization of the Samples. UV/vis diffuse reflectance spectra were recorded in a Shimadzu UV-2101 PC scanning spectrophotometer using an integration sphere. These spectra were compared with those obtained by dissolving Th in H_2SO_4 (96%). EPR measurements were obtained at room temperature using a Bruker spectrometer. IR spectra were carried out at room temperature in a greaseless quartz cell fitted with CaF_2 windows, using a Nicolet 710 FT-IR spectrophotometer after outgassing for 1 h under vacuum (10^{-2} Pa) sequencially at room temperature, 373, 473, 573, and 673 K. IR Spectra of Th and $Th^{\bullet+}BF_4^-$ were carried out in Fluorolube perfluorinated hydrocarbon emulsion. For pyridine adsorption measurements, the wafers (ca. 10 mg) were previously treated under vacuum (10^{-2} Pa) at 673 K for 1 h; pyridine vapor (6.6×10^2 Pa) was then admitted into the cell at room temperature and outgassed under vacuum for 1 h at 423, 523, and 623 K, successively. Thermogravimetric analyses–differential scannning calorimetries were performed with a Netzsch-STA 409 EP thermobalance under air atmosphere.

Results and Discussion

A series of acid zeolites was chosen in order to encompass a representative range of geometrical topolo-

(21) Ramamurthy, V. *Chimia* **1992**, *46*, 359–376.
(22) Gessner, F.; Olea, A.; Lobaugh, J. H.; Johnston, L. J.; Scaiano, J. C. *J. Org. Chem.* **1989**, *54*, 259–261.
(23) Ramamurthy, V.; Eaton, D. F.; Caspar, J. V. *Acc. Chem. Res.* **1992**, *25*, 299–306.
(24) Davis, M. E. *Acc. Chem. Res.* **1993**, *26*, 111–115.
(25) Fava, A.; Sogo, P. B.; Calvin, M. *J. Am. Chem. Soc.* **1957**, *79*, 1078–1083.
(26) Lucken, E. A. C. *J. Chem. Soc.* **1962**, 4963–4965.
(27) Shine, H. J.; Piette, L. *J. Am. Chem. Soc.* **1962**, *84*, 4798–4806.
(28) Murata, Y.; Shine, H. J. *J. Org. Chem.* **1969**, *34*, 3368–3372.
(29) Boduszek, B.; Shine, H. J. *J. Org. Chem.* **1988**, *53*, 5142–5143.
(30) Corma, A.; García, H.; Iborra, S.; Primo, J. *J. Catal.* **1989**, *120*, 78–87.
(31) Pérez-Pariente, J.; Martens, J.; Jacobs, P. A. *Appl. Catal.* **1987**, *31*, 35.
(32) Fajula, F.; Ibarra, R.; Figueras, F.; Gueguen, C. *J. Catal.* **1984**, *89*, 60.
(33) Argauer, R. J.; Landlolt, G. R. U.S. Patent 3,702,886, 1982.
(34) Beck, J. S.; Vartuli, J. C.; Roth, W. J.; Leonowicz, M. E.; Kresge, C. T.; Schmitt, K. D.; Chu, C. T.-W.; Olson, D. H.; Sheppard, E. W.; McCullen, S. B.; Higgins, J. B.; Schlenker, J. L. *J. Am. Chem. Soc.* **1992**, *114*, 10834–10843.
(35) Rubin, M. K.; Chu, P. U. S. Patent 4,954,325, 1990.
(36) Dessau, R. M.; Partridge, R. D. U. S. Patent 4,962,250, 1990.
(37) Corma, A.; Corell, C.; Llopis, F.; Martínez, A.; Pérez-Pariente, J. *Appl. Catal.: A* **1994**, *115*, 121–125.

Table 1. Main Physicochemical Parameters of the Zeolites Used in This Work

zeolite	Si/Al molar ratio	NaO_2 content (%)	crystal size (μm)	BET surface area ($m^2 \times g^{-1}$)	Brönsted/Lewis estimate[a]	channel dimens (Å)
NaY	2.6	11.8	0.8	900	*b*	7.4[c]
CsY	2.6	0.02	0.8		*b*	7.4[c]
HY-100	2.6	<0.01	0.8	750	1:1	7.4[c]
HYD	15	0.03	0.4–0.6	780	2.2:1	7.4[c]
HYD-W	17	<0.01	0.4-0.6		>10:1	7.4[c]
Hβ	13	0.02	0.15	600	1:2	7.6 × 6.4[c]
HMor	10	0.02		550	1.5:1	6.5 × 7.0
HOff[d]	4.26	<0.01		420	1:1	6.7
HZSM-5	17.5	0.05	1–3	430	2:1	5.3 × 5.6
silicalite	>100	<0.01	2–5		*b*	5.3 × 5.6
ZSM-12	96.7	0.51	0.21	240	5:1	5.5 × 5.9
MCM-22	13.6	0.1	0.3	450	1:1.5	
MCM-41	11.3	<0.01		928	1:10	30

[a] Measured as the intensity ratio of the 1550/1450 cm^{-1} absorption bands of the pyridine IR spectra after vapor adsorption at room temperature and subsequent desorption at 523 K under 0.1 Pa for 1 h. [b] No measurable acidity. [c] Supercage dimensions for Y and β zeolites are 13 and 12 Å, respectively. [d] Off stands for offretite.

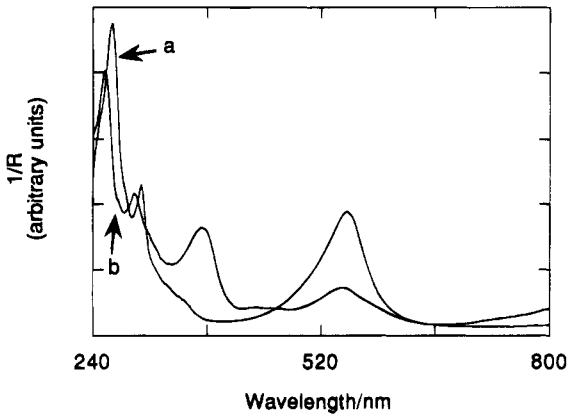

Figure 2. Diffuse reflectances (plotted as the inverse of the reflectivity, $1/R$) of Th-Hβ (a), and Th-HMor (b) composites obtained by Th adsorption from isooctane at 363 K. The band at 550 nm in the visible is characteristic of $Th^{\bullet+}$. For the values of wavelength maxima see Table 2.

gies. Thus, besides the classically available[38–40] faujasites, β , offretite, mordenite, ZSM-5 and ZSM-12, the recently synthesized multidimensional zeolite MCM-22[37,41] and the mesoporous crystalline aluminosilicate MCM-41[24,34,42,43] were also included in this study. Throughout this work, acidity of the samples was characterized according to the pyridine adsorption–desorption method.[44] The main physicochemical parameters of the zeolites studied are summarized in Table 1.

Two different procedures for the incorporation of Th onto the solids by free diffusion from organic solutions or by sublimation from the vapor phase were used in this work.

Adsorption of Th from Organic Solutions. Initially, adsorption of Th onto the solids was carried out at 363 K in isooctane as the organic phase. In a number of cases, the solids became immediately pink to deep blue in color. This indicated that electron transfer processes were occurring during the incorporation of Th. Although the experimental conditions were exactly the same for all the zeolites, the corresponding diffuse reflectances (DR) were strongly dependent on the chemical composition and crystalline structure of the host, as well as the Th concentration.

Thus, the presence of the band at about 550 nm observed in the DR of the Th-Hβ and Th-HMor samples (see, for instance, Figure 2) firmly established the formation of $Th^{\bullet+}$ during the adsorption. However, the other two bands characteristic of $Th^{\bullet+}$ in the UV region at 270 and 290 nm are indistinguishable in the DR of these samples. This may be attributable to the presence of unreacted Th, whose 260 nm absorption maximum obscures the zone, or to the formation of other byproducts during the adsorption procedure.

A reasonable estimation of the relative ratio $Th^{\bullet+}$/Th can be obtained by comparing the intensities of the 550 and 260 nm bands. In addition, the total amount of organic material present on each solid was obtained by thermogravimetric analysis of the samples. These values are collected in Table 2.

In contrast to Th-Hβ and Th-HMor, the visible region of the DR spectra corresponding to the adsorption of Th onto faujasites presented several resolved bands (Figure 3). While the 550 nm band was still attributable to $Th^{\bullet+}$, there are two additional maxima at 465 and 620 nm that, according to the literature, can be assigned to diamagnetic $Th^{\bullet+}$ aggregates.

Such aggregates have been observed in homogeneous media at high concentrations of Th.[26–28,45,46] Although their formation depends on the fourth exponential of the $Th^{\bullet+}$ concentration,[46] their dimeric nature has been proposed assuming that monomeric $Th^{\bullet+}$ perchlorate would be fully dissociated in acetonitrile, while aggregates should exist as ion pairs. It is remarkable that despite working under the same conditions with all the zeolites, these aggregates were observed only using three-dimensional large pore zeolites as hosts. This fact would indicate that they can be accommodated exclusively within the large cavities (11–14 Å) of Y and β zeolites and certainly rule out a sandwich tetrameric nature for these species, dimers being a plausible

(38) Breck, D. W. *Zeolite Molecular Sieves: Structure, Chemistry and Use*; John Wiley and Sons: New York, 1974.
(39) Meier, W. M.; Olson, D. H. *Atlas of Zeolite Structure Types*; Butterworth: London, 1992.
(40) *Introduction to Zeolite Science and Practice*; van Bekkum, H.; Flanigen, E. M.; Jansen, J. C., Ed.; Elsevier: Amsterdam, 1991.
(41) Leonowicz, M. E.; Lawton, J. A.; Lawton, S. L.; Rubin, M. K. *Science* **1994**, *264*, 1910–1913.
(42) Kresge, C. T.; Leonowicz, M. E.; Roth, W. J.; Vartuli, J. C.; Beck, J. S. *Nature* **1992**, *359*, 710–712.
(43) Behrens, P.; Haak, M. *Angew. Chem., Int. Ed. Engl.* **1993**, *32*, 696–699.
(44) Arribas, J.; Corma, A.; Fornés, V. *J. Catal.* **1984**, *88*, 374–380.
(45) Sato, Y.; Kinoshita, M.; Sano, M.; Akamatu, H. *Bull. Chem. Soc. Jpn.* **1969**, *42*, 548.
(46) de Sorgo, M.; Wasserman, B.; Szwarc, M. *J. Phys. Chem.* **1972**, *76*, 3468–3471.

Table 2. Relevant Properties of Some of the Th-H-Zeolite Composites Prepared in This Study

composite	preparation procedure[a]	loss of wt (%) RT−200 °C[b]	loss of wt (%) 400−600 °C[c]	rel $Th^{\bullet+}$/Th estimated[d]	diffuse reflectance λ_{max} (nm)	loading level Th per supercage	loading level Th per acid site[e]
Th-HY-100	S	12.4	13.0	0.04	260, 310, 385, 480, 570, 620	1.00	0.14
Th-HYD	S	10.3	7.5	0.07	265, 305, 380, 465, 560, 620	0.58	0.37
	Sf	10.4	4.7	0.12	260, 300, 555	0.36	0.23
Th-HYD-W	S	14.4	6.3	0.16	265, 390, 475, 570, 620	0.48	0.31
Th-Hβ	S	12.1	3.6	0.39	260, 290, 430, 570	0.12	0.16
	Sg	10.8	4.7	0.37	265, 305, 470, 590	0.15	0.23
	V	9.0	4.1	0.42	260, 290, 545	0.14	0.18
Th-HMor	S	6.7	3.0	0.49	255, 270, 290, 370, 570		0.15
	V	7.4	5.8	>10	270, 290, 545		0.21
Th-HOff[h]	V	12.4	4.2	0.79	270, 280, 300, 550		0.07
Th-HZSM-5[h]	V	6.1	2.1	>10	280, 300, 540		0.12
Th-ZSM-12[h]	V	9.8	3.1	0.36	270, 300, 540		0.18
Th-MCM-22[h]	V	10.2	3.9	0.13	265, 545		0.18
Th-MCM-41	V	16.8	3.5	0.12	265, 550		0.12

[a] S: from isooctane solution (ca. 2.5×10^{-2} M). V: from vapor phase. [b] This column is associated to the amount of water. [c] These values correspond to the amount of organic guest (Th + $Th^{\bullet+}$ aggregates). [d] Intensity ratio of the 550/260 bands in the DR. [e] For nontridirectional zeolites. [f] Using cyclohexane as solvent. [g] Th concentration of the isooctane solution was ca. 1.2×10^{-1} M. [h] No adsorption took place from isooctane solutions.

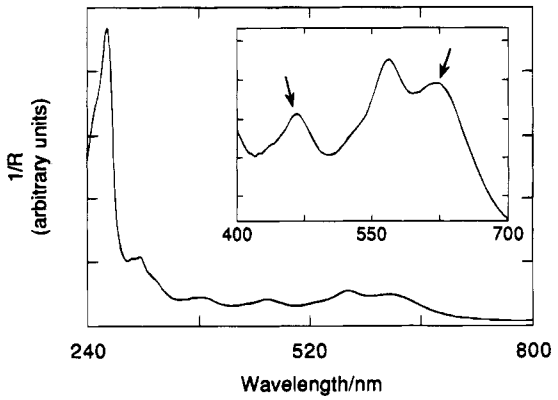

Figure 3. Diffuse reflectance ($1/R$) of Th-HYD composite prepared from isooctane under the same conditions as Figure 1. The inset corresponds to the original spectrum multiplied by a factor of 10. The bands with arrows are characteristic of $Th^{\bullet+}$ aggregates. The wavelengths of the peaks are presented in Table 2.

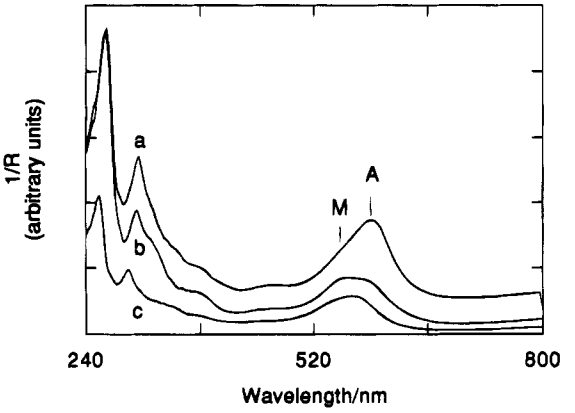

Figure 4. Diffuse reflectance ($1/R$) of a series of Th-Hβ composites prepared using solutions of Th in isooctane at increasing concentration. The curves have been shifted in the $1/R$ axis. The following values correspond to the amount of organic material: (a) 4.69%; (b) 3.97%; (c) 3.59%. The letters M and A indicate the wavelength characteristics of $Th^{\bullet+}$ monomer and aggregate, respectively.

possibility. Firm experimental evidence showing that two tricyclic aromatic hydrocarbons can be assembled within the faujasite supercages has been previously reported.[15,47-49]

The predominant location of Th within the internal voids of these microporous solids can also be inferred from the exiguous formation of $Th^{\bullet+}$ using offretite, ZSM-12, MCM-22, or HZSM-5, barely in the detection limit of the DR technique, although large enough to be fully characterized by EPR. However, the ability of this HZSM-5 sample to generate related cation radicals by adsorption from isooctane solutions of less bulky precursors such as phenylenediamine derivatives has to be remarked.[50,51] These facts indicate that the electron acceptor sites of the zeolites are mainly located in the internal surface. Otherwise no such differences associated to small variations of the zeolite pore diameter or guest molecular size should be observed.

Taking into account the similar cavity dimensions of tridirectional large pore Y and β, we were interested in disclosing whether it is possible to observe dimeric aggregates in the latter structure. As can be seen in Figure 4, absorption bands attributable to the aggregates could also be detected using β as host, although at Th concentrations 3−5 times higher than in the case of faujasites. It is noteworthy that the maximum of this species displayed a 20-nm hipsochromic shift for the β host compared to the Y zeolite. Both facts, the requirement of higher concentrations and the shift of the absorption maximum, could reflect the confinement of the dimer within a tight space. Related precedents about modification of the electronic (absorption or emission) spectra by adsorption within zeolites can be found in the literature.[52-54]

Predictions based on molecular modeling[55] agree well with spatial restrictions as being responsible for the poor

(47) Ramamurthy, V.; Sanderson, D. R.; Eaton, D. F. *J. Am. Chem. Soc.* **1993**, *115*, 10438−10439.
(48) Yoon, K. B.; Kochi, J. K. *J. Am. Chem. Soc.* **1989**, *111*, 1128−1130.
(49) Yoon, K. B.; Huh, T. J.; Corbin, D. R.; Kochi, J. K. *J. Phys. Chem.* **1993**, *97*, 6492−6499.
(50) Generation of Wurster's radical cation by adsorption of *N,N,N',N'*-tetramethyl-*p*-phenylenediamine onto HZSM-5 was ascertained by DR. Results will be published at a latter time.
(51) Roth, H. D. *Tetrahedron* **1986**, *42*, 6097−6100.
(52) Ramamurthy, V. In *Photochemisty in Organized and Constrained Media*; V. Ramamurthy, V., Ed.; VCH: New York, 1991; Chapter 10, pp 429−493.
(53) Haley, J. L.; Fitch, A. N.; Goyal, R.; Lambert, C.; Truscott, T. G.; Chacon, J. N.; Stirling, D.; Schalch, W. *J. Chem. Soc., Chem. Commun.* **1992**, 1175−1176.
(54) Cozens, F. L.; García, H.; Scaiano, J. C. *Langmuir* **1994**, *10*, 2246−2249.

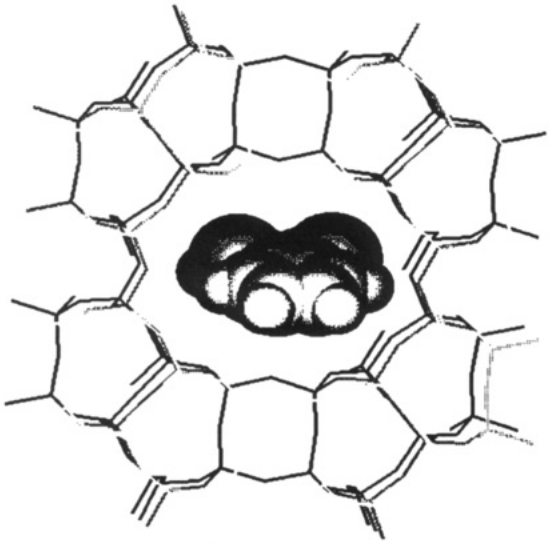

Figure 5. Molecular modeling of Th incorporated within the channels of mordenite showing the arrangement for which host−guest van der Waals interactions are prevented. Docking calculations indicate that deviations from this arrangement result in a severe overlap of guest/host van der Waals radii.

adsorption of Th in HZSM-5, as well as for the dimeric nature of Th aggregates within Y and β zeolites. A visualization of Th hosted within the channels of mordenite is provided in Figure 5.

When the isooctane solutions used for the incorporation of Th onto the hosts were analyzed, products of an unexpected reaction were detected. Again, a clear relationship between the void dimensions of the host and the outcome of this reaction was observed. Thus, in the case of mordenite the recovered material was predominantly (>90%) unreacted Th; by contrast, when Y zeolites were used the major product was the *tert*-butylthianthrene. Besides, an extremely complex mixture of alkanes was formed, as evidenced by GC-MS analysis.

An intermediate situation was observed for Hβ , where the *tert*-butylation of Th occurred to a lower extent. As shown in Figure 5, the tight fit of Th within the reaction cavity[56] precludes (mordenite), or makes it difficult (β), its reaction with the solvent. This reaction is rather surprising, since isooctane has been widely used as an inert liquid phase for the incorporation of organic guests within zeolite media.[22,57,58] We addressed the possibility that *tert*-butylthianthrene arises from C-alkylation of Th by *tert*-butyl cation (presumably generated by cracking of isooctane on the acid sites). However, this possibility was ruled out since treatment of *tert*-butyl alcohol and Th in H_2SO_4 or in the presence of HY-100 at reflux temperature even for extended periods of time only led to very minor amounts of *tert*-butylthianthrene accompanied by unaltered Th. Thus, our finding must be the result of highly specific electron transfer processes occurring during Th adsorption within acid zeolites. Although it is well known that $Th^{\bullet+}$ is able to promote chemical reactions,[28,59−63] producing sometimes Th derivatives,[59,61,62] *tert*-butylation of Th is unprecedented, probably due to the lack of solubility of $Th^{\bullet+}$ salts in isooctane.

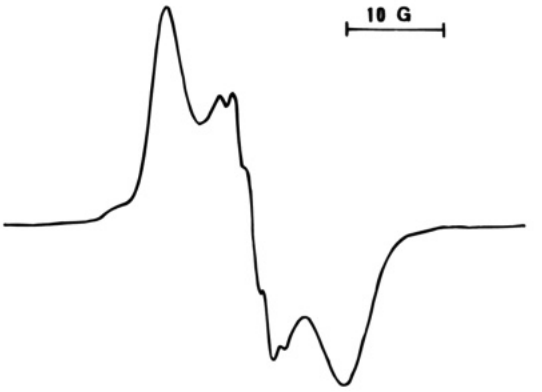

Figure 6. Electron spin resonance recorded at room temperature of a Th-HMor composite prepared from isooctane solution. Note that only trace amounts of *tert*-butylated thianthrene is formed in this case.

In addition, the yield of *tert*-butylthianthrene enables an estimation of the minimum amount of $Th^{\bullet+}$ formed in the acid Y and β samples, which is at least 0.01 mmol/g of zeolite (about 10^3 times higher than the value previously calculated for Na^+-ZSM-5 using α,ω-diphenylpolyenes[6]).

The nature of the solvent was a key factor in the generation of $Th^{\bullet+}$. Thus, using acetonitrile resulted in an apparent decrease of the Th uptake as well as the electron acceptor ability of the solids, as assessed by the weight of recovered Th and the variations in the relative intensity of DR bands corresponding to $Th^{\bullet+}$ and Th. This fact might reflect solvent competition either for the oxidizing sites or simply for the zeolite internal surface.[64,65] Cyclohexane was found to be a very convenient inert solvent to generate $Th^{\bullet+}$.

Further characterization of Th incorporated within zeolites was accomplished by EPR and FT-IR spectroscopy. The former technique showed at room temperature the expected signal attributable to $Th^{\bullet+}$ [66−68] (Figure 6). It is worth noting that the typical hyperfine splitting of $Th^{\bullet+}$ spectrum using conventional solvents appeared in our samples overlapped onto a broader unresolved band with apparently the same g value, whose origin is uncertain at the present. However, it is noticeable that reported EPR spectra of $Th^{\bullet+}ClO_4^-$ and $Th^{\bullet+}SbCl_6^-$ in solid state show remarkable distorted signals.[26] Furthermore, it has been found that the EPR spectrum of $Th^{\bullet+}$ looses its symmetry and hyperfine

(55) Docking using the Biosym Insight II Molecular Modeling package running on a Silicon Graphics workstation.
(56) Weiss, R. G.; Ramamurthy, V.; Hammond, G. S. *Acc. Chem. Res.* **1993**, *26*, 530−536.
(57) Turro, N. J.; Cheng, C.-C.; L., A.; Corbin, D. R. *J. Am. Chem. Soc.* **1987**, *109*, 2449−2456.
(58) Full experimental details comparing the aromatic alkylation of thianthrene and anthracene by *tert*-butyl alcohol in the presence of acid zeolites will be published elsewhere.

(59) Shine, H. J.; Yueh, W. *J. Org. Chem.* **1994**, *59*, 3553−3559.
(60) Kim, K.; Hull, V. J.; Shine, H. J. *J. Org. Chem.* **1974**, *39*, 2534−2539.
(61) Shine, H. J.; Yueh, W. *Tetrahedron Lett.* **1992**, *33*, 6583−6586.
(62) Shin, S.-R.; Shine, H. J. *J. Org. Chem.* **1992**, *57*, 2706−2710.
(63) Engel, P. S.; Robertson, D. M.; Schulz, J. N.; Shine, H. J. *J. Org. Chem.* **1992**, *57*, 6178−6187.
(64) It has been found that organic guest uptake onto zeolites is more efficient if apolar solvents are used.
(65) Ramamurthy, V.; Caspar, J. V.; Eaton, D. F.; Kuo, E. W.; Corbin, D. R. *J. Am. Chem. Soc.* **1992**, *114*, 3882−3892.
(66) Shine, H. J.; Dais, C. F.; Small, R. J. *J. Org. Chem.* **1964**, *29*, 21−25.
(67) Shine, H. J.; Sullivan, P. D. *J. Phys. Chem.* **1968**, *72*, 1390−1391.
(68) Sullivan, P. D. *J. Am. Chem. Soc.* **1968**, *90*, 3618−3622.

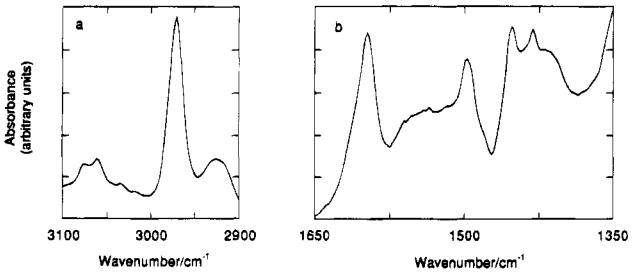

Figure 7. C–H stretching bands (a) and aromatic region (b) of the IR spectrum of Th-Hβ composite after outgassing under 10^{-2} Pa at 473 K for 1 h. This sample was prepared by Th adsorption from isooctane solution.

structure when this species is photochemically generated onto layered clay surfaces.[69]

IR spectroscopy was found to be an especially powerful technique to get a better knowledge of these samples. Thus, the IR spectra of the composites after outgassing under vacuum at different temperatures clearly revealed the presence of adventitious organic material, as evidenced by the intense aliphatic C–H vibration bands below 3000 cm^{-1}, and the presence of broad unresolved bands in the aromatic region. These facts were observed even in the IR spectra of samples prepared using cyclohexane as solvent, where no reaction products could be detected. A typical spectrum is presented in Figure 7.

Adsorption of Th from the Vapor Phase. Incorporation of Th into acid zeolites from organic solutions was found to be a rather complex process. Thus, besides generation of $Th^{\bullet+}$ and the presence of unreacted Th, other byproducts must be formed as revealed by the UV region of the DR spectra, the presence of solvent derived products in the organic solutions recovered after extraction, and unexpected observation of functional groups in the IR spectra.

It was thought that many of these problems arise from the use of a solvent. Taking into account that Th sublimes at low temperatures, adsorption of Th was carried out from the vapor phase. It was found that the most simple and convenient procedure was heating progressively up to 473 K a mixture of Th and zeolite under Ar stream.

Working under these conditions, DR of the composites exhibited in the UV region the characteristic doublet at 270 and 290 nm previously reported in the UV/vis absorption spectrum of $Th^{\bullet+}$ in solution. As can be seen in Figure 8, even the 260 nm band due to unreacted Th was absent in Th-HMor samples where loadings of Th between 1 and 6 wt % were used. Furthermore, the bands associated with formation of aggregates were not observed with this methodology even in the case of large (Y, β) or extralarge pore (MCM-41) samples.

IR spectroscopy also confirmed that vapor phase adsorption yields in several cases clean composites containing exclusively $Th^{\bullet+}$. Surprisingly, the IR spectrum of $Th^{\bullet+}$ cannot be found in the literature. Previous attempts to get the IR in KBr disk led to the spectrum corresponding to the neutral Th precursor, with simultaneous generation of bromine.[26] Herein, we have recorded the spectrum of the $Th^{\bullet+}BF_4^-$ salt in an inert perfluorinated matrix. This tetrafluoroborate salt was

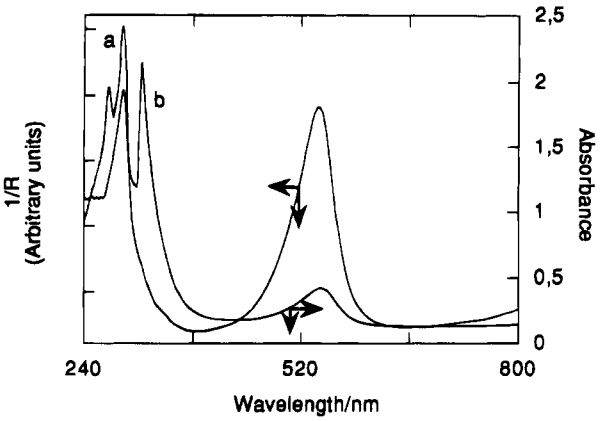

Figure 8. Diffuse reflectance ($1/R$, left axis, curve a) of the Th-HMor composite prepared by the vapor phase adsorption. Curve b shows the UV/vis absorption spectrum (absorbance, right axis) of $Th^{\bullet+}$ prepared by dissolving Th in 96% H_2SO_4.

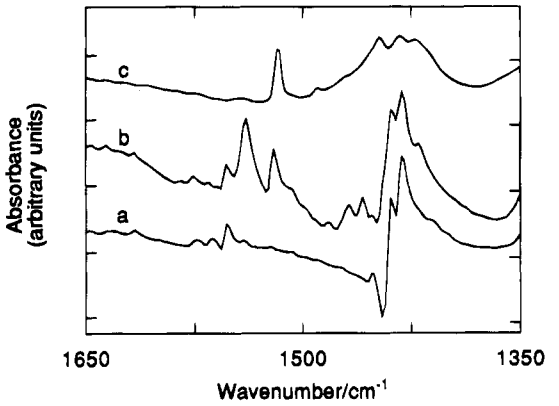

Figure 9. Aromatic region of the IR spectra of Th (a) and $Th^{\bullet+}BF_4^-$ (b) in Fluorolube emulsions. Curve c corresponds to the IR spectrum of Th-Hβ composite prepared by the vapor phase adsorption method recorded at room temperature after outgassing the sample under 10^{-2} Pa at 473 K for 1 h. The traces have been shifted along the absorbance axis, while plot c corresponds to half the intensity of the original spectrum of Th-Hβ.

prepared by the $NO^+BF_4^-$ oxidation method,[29] and its purity determined by iodometric titration was 84%.

For the sake of comparison, Figure 9 contains the FT-IR spectra of Th, $Th^{\bullet+}BF_4^-$ and that of the Th-Hβ sample obtained after outgassing at 473 K for 1 h. As can be seen the last spectrum can be confidently assigned to $Th^{\bullet+}$. It appears that the band at 1518 cm^{-1}, absent in the spectrum of Th, can be associated specifically to $Th^{\bullet+}$ for identification purposes.

Moreover, no intensity changes of the characteristic 1518 cm^{-1} band were observed after desorbing the composites under vacuum from room temperature to 573 K. This would indicate that $Th^{\bullet+}$ is strongly adsorbed onto the solids. Thermogravimetric profiles of these composites also corroborated this point. In addition, comparison of these spectra with those of the original acid zeolites before any adsorption showed an appreciable intensity decrease of the original acidic OH bands (~3600 cm^{-1}). This agrees well with the partial replacement of H^+ by $Th^{\bullet+}$ as countercation.

An important feature of the sublimation method was that offretite, ZSM-12, MCM-22, as well as medium pore HZSM-5, that had previously failed in the adsorption from organic solutions, were able to generate $Th^{\bullet+}$ under vapor phase adsorption conditions. The same was true

(69) Mao, Y.; Thomas, J. K. *J. Org. Chem.* **1993**, *58*, 6641–6649.

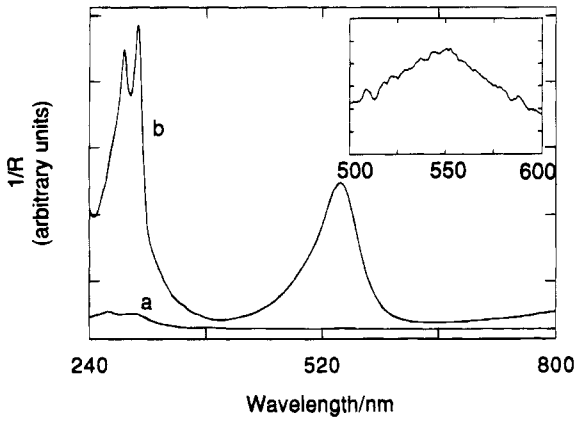

Figure 10. Diffuse reflectances (1/*R*) of two Th-HZSM-5 samples prepared by adsorption from a solution of isooctane at 363 K (a) and from the vapor phase at 473 K (b), respectively. The inset corresponds to trace a multiplied by a factor of 20.

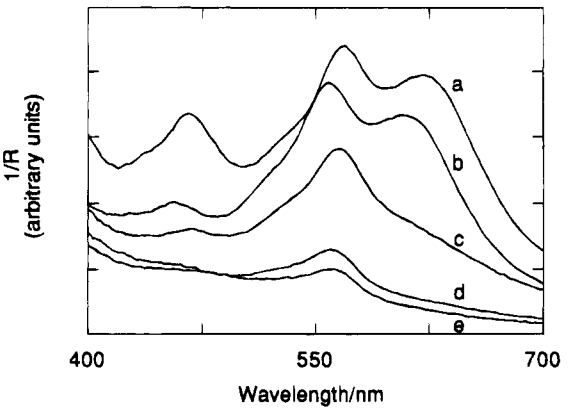

Figure 11. Reflectance (1/*R*) changes in the 400–700 nm region with the elapsed time of Th-HY composite stored at ambient atmosphere. The original spectrum corresponds to trace a, while curves b, c, d, and e were recorded after 1, 2, 5, and 20 days, respectively.

for the extralarge pore zeotype MCM-41, where the sublimation method was successful, while adsorption from Th solutions also failed, probably because of an easy reacction of $Th^{\bullet+}$ with adventitious water (see below). Figure 10 provides a comparison of the different results attained with HZSM-5 depending on the experimental procedure. These discrepancies can be easily interpreted as due to an enhancement of Th diffusion through the internal micropores of the zeolite crystal under the conditions of the vapor phase adsorption. Besides the absence of solvent, the higher adsorption temperature (473 K instead of 363 K) would increase the vibration of the lattice and the kinetic energy, thus reducing diffusional restrictions. In fact, molecular simulation presented in Figure 5 assumes that no vibration of the lattice are taking place.

Aging of the Th-HZeol Composites: Influence of Water and Oxygen. When the zeolites containing $Th^{\bullet+}$ were kept for several months under anhydrous conditions, the recorded DR were exactly the same as those obtained immediatly after the preparation. However, samples stored at the open air progressively lose their color, and the characteristic 550-nm band completely disappeared within days. It was noticeable that in the case of Y samples containing $Th^{\bullet+}$ dimers, these aggregates decayed faster than monomeric $Th^{\bullet+}$ (Figure 11). In this connection, the influence of water content on the aggregation of similarly shaped thionine within zeolite Y has been already reported.[47]

To get a better understanding of this aging process, freshly prepared Y and β samples by vapor adsorption of Th were submitted at room temperature to a H_2O-saturated N_2 stream. Under these conditions $Th^{\bullet+}$ disappeared within minutes. However, purge with dry N_2 at 310 K was enough to regenerate again the same amount of $Th^{\bullet+}$, as evidenced by DR technique. Three consecutive cycles did not produce any significant reduction aging.

Reaction of $Th^{\bullet+}$ with H_2O to give thianthrene oxide (ThO) has been the subject of numerous studies.[27,69,70,71] In the case of $Th^{\bullet+}$ hosted within zeolites, the observed reversibility under the very mild conditions employed does not fit well with the occurrence of a chemical reaction leading to ThO. Rather than covalent bond changes, our results suggest that *complexation* of H_2O with $Th^{\bullet+}$ or with the surface oxidizing sites must be the process responsible for the observed decay of the radical cation. In fact, after complete disappearance of $Th^{\bullet+}$ only minor amounts of ThO were observed after exhaustive Sohxlet extraction of the solids, which allowed the recovery of the unaltered Th with excellent mass balances. This result is in line with recent reports on H_2O interaction with photogenerated $Th^{\bullet+}$ onto clay surfaces.[69] Of the three general reaction mechanisms followed by organic radical cations,[72] only recently a consensus has been reached that the first step involves the reversible formation of a complex between H_2O and $Th^{\bullet+}$.[73,74] Therefore, we suggest that aging of the composites begins with some complexation equilibrium, which can be reversed at initial stages by removal of H_2O.

The role played by oxygen as a possible electron sink during the generation of radical cations by zeolites has been already postulated.[1,75] In our case, $Th^{\bullet+}$ could be positively formed under Ar atmosphere. However, working under O_2 or ulterior treatment of $Th^{\bullet+}$-HMor with an O_2 stream gave rise to a remarkable increase of the absorption bands corresponding to $Th^{\bullet+}$. These observations parallel those observed in homogeneous solutions using trifluoroacetic acid, where the absence of oxygen almost, but not entirely, supress $Th^{\bullet+}$ formation.[27] In fact, other radical cations of polynuclear aromatics[76] and biphenylenes[77] cannot be generated in trifluoroacetic acid unless oxygen is admitted.

Nature of Zeolite Oxidizing Sites. To disclose the nature of the oxidizing sites responsible for the electron acceptor ability, Th was adsorbed onto a series of zeolites submitted to Na^+ or Cs^+ exchange, dealumination, or washing with ammonium hexafluorosilicate.

(70) Hammerich, O.; Parker, V. D. *Acta. Chem. Scand. B* **1982**, *36*, 421–433.
(71) Parker, V. D. *Acc. Chem. Res.* **1984**, *17*, 243–250.
(72) Hammerich, O.; Parker, V. D. *Adv. Phys. Org. Chem.* **1984**, *20*, 55–189.
(73) Jones II, G.; Huang, B. *Tetrahedron Lett.* **1993**, *34*, 269–272.
(74) Jones II, G.; Huang, B.; Griffin, S. F. *J. Org. Chem.* **1993**, *58*, 2035–2042.
(75) Yudanov, I. V.; Zakharov, I. I.; Zhidomirov, G. M. *React. Kinet. Catal. Lett.* **1992**, *48*, 411–417.
(76) Aalsbersberg, W. J.; Hoijtink, G. J.; Mackor, E. L.; Weijland, W. P. *J. Chem. Soc.* **1959**, 3049.
(77) Ronlan, A.; Parker, V. D. *Chem. Commun.* **1974**, 33.

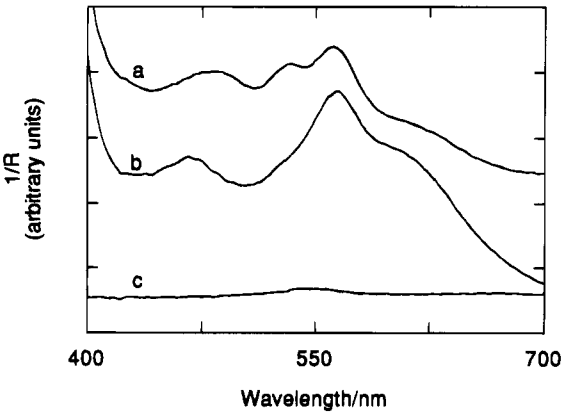

Figure 12. Diffuse reflectance ($1/R$) of Th-HY-100 (a), Th-HYD-W (b), and Th-HY-100N (c) samples prepared under the same experimental conditions.

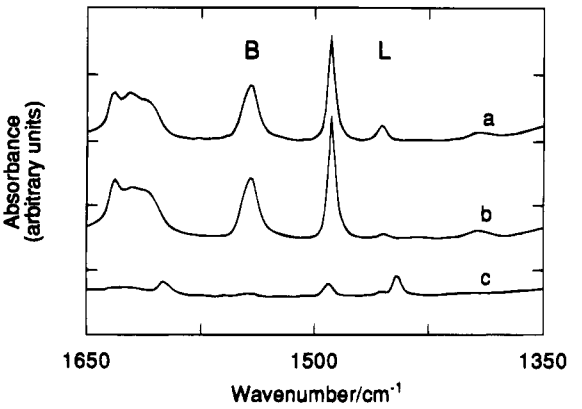

Figure 13. IR spectra at room temperature of pyridine adsorbed on HY-100 (a), HYD-W (b), and HY-100N (c) after desorption at 473 K for 1 h. The letters B and L indicate the specific bands due to Brönsted and Lewis sites, respectively. Note the low intensity of Lewis coordinated pyridine band at 1450 cm^{-1} in spectrum b and the absence of Brönsted band at 1500 cm^{-1} in case c.

Thus, nonacidic NaY, CsY, or silicalite (see Table 1) failed to generate $Th^{\bullet+}$. Moreover, the ability of the HY-100 sample to generate $Th^{\bullet+}$ was lost when this solid was submitted to an exhaustive H^+-to-Na^+ exchange (HY-100N). On the other hand, the ability to generate $Th^{\bullet+}$ remained essentially unaltered when extraframework aluminum (EFAL, responsible for the Lewis acidity[78]) of a dealuminated Y zeolite was totally removed by continued washings with $(NH_4)_2SiF_6$ (HYD-W) (Figure 12).[79]

Characterization of the resulting HY-100N by the pyridine method[44] showed that all Brönsted sites had been neutralized, while Lewis sites were still present. The reverse was true for HYD-W sample which was shown to contain only Brönsted acid sites (Figure 13). Similarly, a purely Lewis acid solid such as silica–alumina was found to be inactive to form $Th^{\bullet+}$ under our experimental conditions.

This finding may seem contradictory with the reported generation of $Th^{\bullet+}$ using conventional Lewis acids. However, since the reaction mechanism has not yet been established, our result may reflect the different nature or strength of zeolite Lewis sites.

Conclusions

Thianthrene has been used as a probe molecule to show that electron transfer processes may in general occur during the incorporation of organic guests within acid zeolites, independent of their crystalline structure. UV/vis diffuse reflectance and IR spectroscopy revealed that composites containing pure $Th^{\bullet+}$ can be prepared by the vapor phase adsorption method. This has allowed us to report for the first time the IR spectrum of thianthrene radical cation. In the case of tridimensional large pore zeolites, the formation of dimeric $Th^{\bullet+}$ aggregates can also occur. It has been shown that the electron acceptor ability of these zeolites is mainly due to Brönsted acid sites, associated to bridged Si–(OH)–Al hydroxyls. Generation of $Th^{\bullet+}$ can be carried out under strictly oxygen-free conditions. However, oxygen influences this process, enhancing the population of $Th^{\bullet+}$. On the other hand, ambient moisture is the main factor responsible for the aging of these composites. It has been found that the disappearance of $Th^{\bullet+}$ can be reversed at initial stages by drying the solids under mild conditions. Finally, the vapor-phase incorporation of $Th^{\bullet+}$ within confined spaces opens a new methodology to control the chemistry of this radical cation, as we have shown in the case of the unprecedented reaction with isooctane.

Acknowledgment. Financial support of the Spanish Dirección General de Ciencia y Tecnología (Grant PB93-0380) and the Generalitat Valenciana (fellowship to V.M.) is gratefully acknowledged. Thanks are due to R. Torrero for technical assistance.

CM950214T

(78) Radwglia, R.; Engelhardt, G. *Chem. Phys. Lett.* **1985**, *114*, 28–31.

(79) Corma, A.; Fornés, V.; Rey, F. *Appl. Catal.* **1990**, *59*, 267.